RESEARCH

Effects of discharge tube and coolant materials on longitudinally excited CO_2 laser with fast pulsed discharge

Yasushi Kodama[1,2] · Shohei Watarai[2] · Kazuyuki Uno[1]

Abstract

In diffusion-cooled gas lasers, the laser medium gas is cooled through the discharge tube wall. Empirical findings suggest that, in longitudinally excited CO_2 lasers with fast pulsed discharges, the materials of the discharge tube and coolant impact the discharge. This study investigates their effects on fast discharges rather than on cooling. Within a discharge tube with a cooling tube, the discharge tube and coolant create a capacitor, influencing the discharge. The laser output energy varies based on the discharge tube and coolant materials. The primary discharge input energy is influenced by these materials, as is the efficiency of converting it into laser output energy.

1 Introduction

The CO_2 laser, with a wavelength range of 9.1–12.3 μm, is a gas laser. This wavelength range is readily absorbed by non-metallic materials like resins, ceramics, and biological tissues. Short-pulse CO_2 lasers meet advanced processing needs that have arisen recently, including processing with a small heat-affected zone and selectively processing resin in metal and resin composites.

The most common techniques for short-pulse CO_2 lasers are the transverse excitation (TE) method [1] and the Q-Switch method [2]. However, our focus is on the longitudinally excited (LE) method. Even with the LE method, short-pulse CO_2 lasers can be generated by optimizing the gas mixing ratio and high-speed discharge. We previously reported that the LE-CO_2 laser produced short pulses with a spike pulse width of about 100 ns and a pulse tail of several tens of μs [3], as well as tail-free short pulses with a pulse width of about 100 ns [4]. Using LE-CO_2 lasers, various pulse shapes can be generated by adjusting the gas medium,

even under the same excitation circuit [5]. For CO_2-rich gases at low gas pressures (<2 kPa), a tail-free short pulse with a pulse width of approximately 100 ns is generated, whereas for CO_2-rich gas at high gas pressures (>2 kPa) and N_2-rich gas at low gas pressures (<6 kPa), a short pulse is generated that short pulses containing spike pulses with a pulse width of approximately 100 ns and pulse tails with a length of 10–200 μs are generated. Meanwhile, long laser pulses with a pulse width of 10–20 μs are generated in N_2-rich gas at high gas pressures (>6 kPa). Furthermore, using the LE-CO_2 laser, one can generate doughnut-shaped beams, flat-top beams, and Gaussian beams by appropriately adjusting the resonator [6]. The pulse energy of the LE-CO_2 laser is a few hundred millijoules [5], which is lower than that of the TE-CO_2 laser. The LE method is characterized by its simple configuration, which does not require high-speed gas flow or strong pre-ionization, and its ability to form a circular Gaussian beam easily due to the small circular aperture and long resonator length [7]. This enables the realization of compact laser systems and simple processing optics, making the LE method suitable for small processing equipment used in the production of many models in small quantities.

Based on our market research, the demand for an LE-CO_2 laser with fast pulsed discharge includes high repetition rate operation, ideally ranging from 5 to 10 kHz, to meet market requirements for cycle time. We recently reported on achieving 1 kHz repetition rate operation of the LE-CO_2 laser [7] and investigated the effect of high repetition rates on the discharge characteristics of the LE-CO_2 laser [8]. We are actively pursuing further improvements in repetition rate.

✉ Yasushi Kodama
  y_kodama@sedeco.co.jp

1   Integrated Graduate School of Medicine, Engineering, and Agricultural Sciences, University of Yamanashi, 4-3-11 Takeda, Kofu, Yamanashi 400-8511, Japan

2   Technology and Engineering Division, Seidensha Electronics Co., Ltd, 2-2-17 Nishi-Nippori, Arakawa-ku, Tokyo 116-0013, Japan

Cooling plays a crucial role in enabling high repetition rate operation of CO_2 lasers. Effective cooling reduces the population of CO_2 molecules in the 01^10 level, thereby enhancing excitation efficiency and output power of the laser. In diffusion-cooled gas lasers, the medium gas is cooled through the wall of the discharge tube. Historically, cooling of discharge tubes has utilized air or water, from the earliest reports of CO_2 laser development [9, 10] to recent ones [11, 12]. However, in our LE-CO_2 laser, categorized as a diffusion-cooled laser, we observed a decrease in laser output energy when the discharge tube was cooled with water. This decrease may be attributed to the formation of a capacitor between the water, which has high permittivity, and the discharge tube with a cooling tube, potentially affecting the laser output energy of the fast discharge pumped laser.

This study aims to explore the impact of discharge tube material and coolant material on fast discharge in an LE-CO_2 laser, rather than focusing on their effect on cooling.

2 Experimental setup

Figure 1 depicts a schematic diagram of the experimental setup, which comprised two discharge tubes constructed of dielectric tubes with an inner diameter of 6 mm, an outer diameter of 10 mm, and a length of 400 mm. Electrodes A and B, along with two AR-coated ZnSe windows, were affixed to the ends of each discharge tube. Electrodes A and B were linked to ground via a current balancing transformer to ensure uniform current distribution in both tubes. Electrodes C and D were positioned opposite each other midway along the tubes. The discharge length, spanning from electrode C

(or D) to electrode A (or B), measured 410 mm. Electrode C was connected to a capacitor C1 and a high-voltage power supply, with a large resistor R included for safety. Electrode D was grounded through capacitor C2. Cooling tubes, composed of aluminum with dimensions of 21 mm inner diameter, 25 mm outer diameter, and 260 mm length, enveloped the discharge tubes to facilitate coolant flow. Coolant circulated between the discharge tubes and cooling tubes, with the latter connected to ground. The optical cavity comprised an output coupler crafted from ZnSe with 85% reflectivity and a highly reflective mirror featuring a curvature radius of 5 m. The cavity length measured 956 mm. To enhance beam quality by suppressing the generation of higher-order modes, apertures with diameters of 5.5 mm on the output mirror side and 6.0 mm on the highly reflective mirror side were installed in the cavity. A premixed gas mixture of CO_2:N_2:He = 1:1:5 flowed through the discharge tube, with the gas flow rate regulated by a throttle valve at the inlet. Gas pressure was monitored at the outlet. The power supply generated a high-voltage pulse of approximately 25 kV with a rise time of about 250 ns, resulting in an energy output of roughly 125 mJ. As the charging of capacitor C1 by the high-voltage pulse commenced, a discharge occurred between electrodes C and D, which are closely spaced. This discharge charged capacitor C2 and served as a mechanism to stabilize the starting voltage of the main discharge. When capacitors C1 and C2 reached their charged state and the voltage between electrode C (or electrode D) and electrode A (or electrode B) reached the breakdown threshold, the main discharge occurred within the discharge tube, resulting in laser output. To mitigate heat load on the discharge tube, the repetition rate was set to 10 Hz. Voltages V1 and

Fig. 1 Schematic diagram of experimental setup. W, OC, M, C1, C2, and R represent AR-coated ZnSe window, output coupler, high-reflectivity mirror, 400 pF capacitor, 400 pF capacitor and 2 MΩ resistor, respectively. V1 and V2 are voltage measurement points, and I1 and I2 are current measurement points
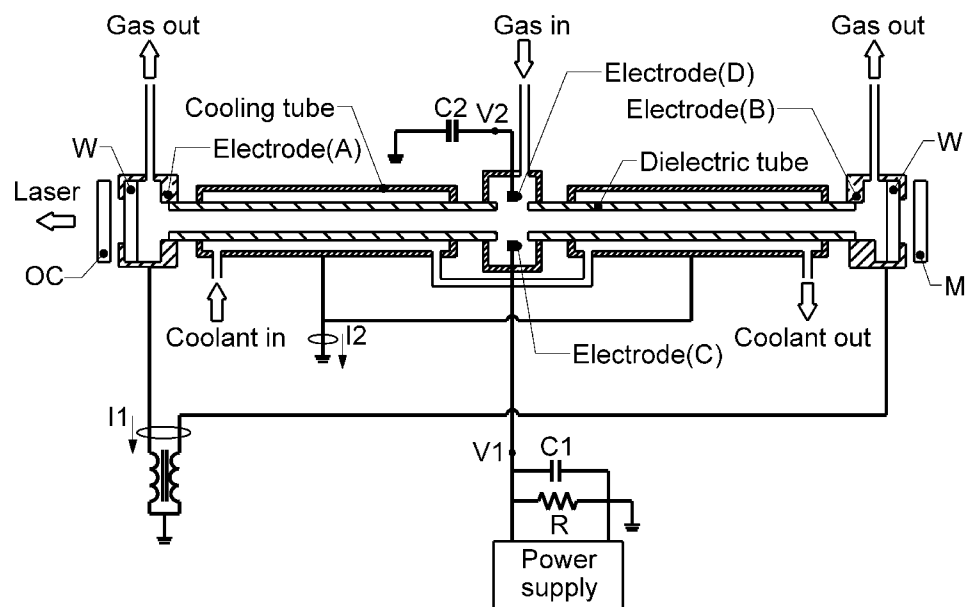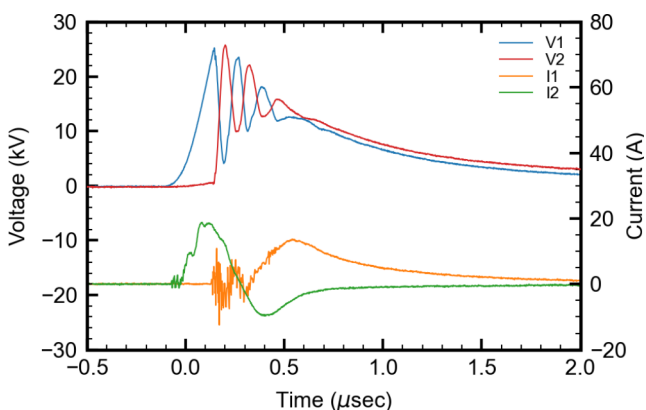
Table 1 Relative permittivity of materials at 1 MHz

material	relative permittivity
alumina ceramic	9.9
borosilicate glass	4.6
fused silica	3.9
pure water	78.6
fluorinated fluid	6.1
air	1.0

Fig. 2 Voltage and current waveforms with an alumina ceramic discharge tube, pure water coolant, and a gas pressure of 3.0 kPa. Blue, red, orange, and green lines correspond to voltage V1, voltage V2, current I1, and current I2, respectively

V2 were measured using a high-voltage probe (Tektronix P6015A), while currents I1 and I2 were measured using a current monitor (PEARSON MODEL110A). Laser pulse waveforms were recorded using an InAsSb photovoltaic detector (Hamamatsu P13894-011MA), and laser output energy was quantified using a power meter (COHERENT PM30). The discharge tubes were constructed of alumina ceramic, borosilicate glass, and fused silica, while the coolants employed were pure water, fluorinated fluid, and air. Pure water and fluorinated fluid were delivered to the cooling pipe at a flow rate of 1.6 l/min, and air was supplied at a pressure of 10 kPaG, with the outlet side open to the atmosphere. Table 1 illustrates the known relative permittivity of each material.

3 Results and discussion

3.1 Effects of cooling structure

We examined the capacitor formed by the discharge tube and coolant. Figure 2 illustrates voltages V1 and V2, and currents I1 and I2 with an alumina ceramic discharge tube, pure water coolant, and a gas pressure of 3.0 kPa. Time 0 marks when voltage V1 hits 20% of its peak value. The high voltage pulse charged capacitor C1 swiftly, causing a rapid rise in voltage V1. As the voltage between electrodes C and D reached breakdown, a discharge path formed between them, leading to oscillatory charge transfer between capacitors C1 and C2, altering voltages V1 and V2. At the breakdown voltage between electrode C (or D) and electrode A (or B), a main discharge ensued from electrodes C and D to electrodes A and B. The breakdown voltage of the main discharge, defined as the maximum of voltages V1 and V2, measured 25.8 kV at 0.2 μs. With a discharge length of 410 mm and gas pressure of 3.0 kPa, the electric field strength-to-gas pressure ratio (E/P) was 20.9 VPa^{-1}m^{-1}. Current I1, flowing through the discharge tube to ground, constituted the main discharge current for laser excitation. Current I2, flowing from the cooling tube to ground, began increasing at the onset of capacitor C1 charging and decreased as charging ceased. The oscillation of current I2 suggested that the discharge tube and coolant formed a capacitor (hereafter referred to as capacitor Cs).

In general, the energy $E(t_1)$ consumed by the load at time t_1 is expressed by the following equation using the voltage $V(t)$ and current $I(t)$.
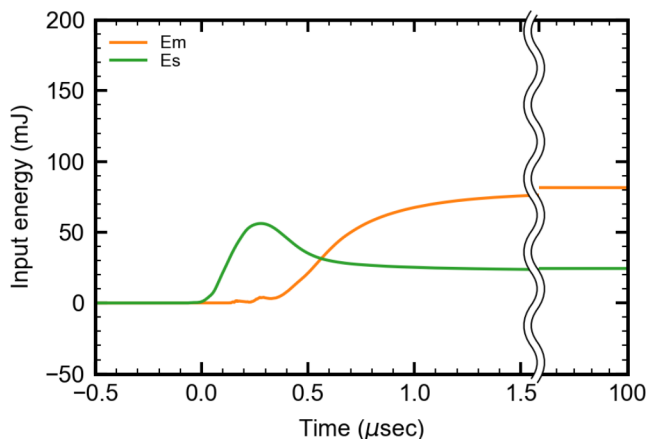
$$E(t_1) = \int_0^{t_1} V(t) \cdot I(t)\, dt$$

Fig. 3 Calculation results of input energy with an alumina ceramic discharge tube, pure water coolant, and a gas pressure of 3.0 kPa. Orange and green lines represent main discharge input energy (Em) and capacitance Cs input energy (Es), respectively

Equation (1) allows us to compute the main discharge input energy using the time waveform of voltage V1 and current I1, while the input energy of capacitor Cs can be determined using the time waveform of voltage V1 and current I2. Figure 3 presents the calculated results of the main discharge input energy and the input energy of capacitor Cs. The main discharge input energy measured 82 mJ per pulse at 100 µs, following a sufficient time period. Meanwhile, the input energy of capacitor Cs peaked at 50 mJ at 0.3 µs, then gradually declined over time, stabilizing nearly constant after 1.5 µs. The 50 mJ stored in capacitor Cs was subsequently released and contributed to the main discharge energy. By 100 µs, after ample time had passed, the input energy of capacitor Cs dwindled to 13 mJ, indicating consumption due to dielectric loss. The energy released by capacitor Cs and utilized for the main discharge amounted to 37 mJ. In essence, out of the 82 mJ main discharge input energy,

37 mJ was provided through the capacitor Cs formed by the discharge tube and coolant.

In this study, a 100 µs threshold was used to indicate sufficient time for the calculations described above. At high gas pressures, electric charge may remain in capacitor C1 due to slower discharge rates. Consequently, even when the time reaches 100 µs, V1 may not reach zero. However, from 50 µs onward, both currents I1 and I2 approach zero. Since zero currents nullify any impact on the energy calculation results, the voltage V1 being non-zero at this stage is inconsequential. Moreover, a comparison of calculation results at 50 µs and 100 µs reveals their near equivalence. Hence, the 100 µs mark was employed in calculating both the main discharge input energy and the dielectric loss energy of capacitor Cs in this paper.

Figure 4 displays the waveforms of the laser pulse and voltage V1 using an alumina ceramic discharge tube, pure water coolant, and gas pressure of 3.0 kPa. Laser oscillation commenced at 1.1 µs. The spikes observed in the laser pulse waveform between 0.1 and 0.7 µs were attributed to switching noise from the main discharge. Specifically, the laser pulse exhibited a spike pulse width of 430 ns and a pulse tail width of 115 µs. For this study, the spike pulse width was determined as the full width at half maximum, while the pulse tail width was defined as the length from the end of the spike pulse to the end of the pulse tail. The laser pulse energy measured 8.0 mJ.

3.2 Effect on laser output energy

The impact of discharge tube material and coolant material on laser output energy was examined. In Fig. 5a, the ratio of electric field strength to gas pressure (E/P) dependence of laser output energy in fused silica discharge tubes is depicted. The coolant material influenced the laser output
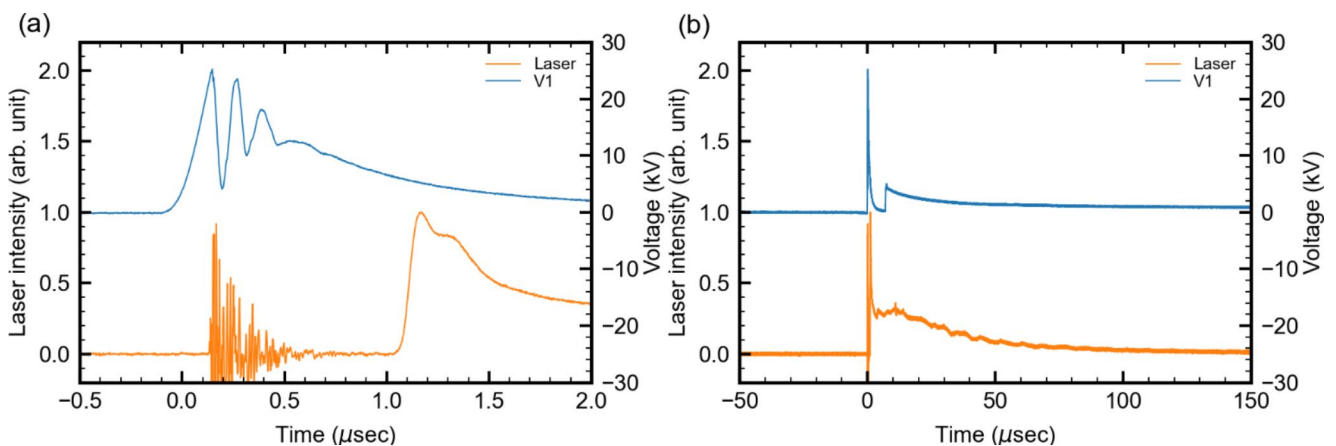

Fig. 4 Laser pulse and discharge voltage waveforms with an alumina ceramic discharge tube, pure water coolant, and a gas pressure of 3.0 kPa. Orange and blue lines represent laser pulse and discharge voltage waveforms, respectively. (**a**) Magnified time-scale view of spike pulse. (**b**) Overall waveform. (The discharge voltage waveform is similar to the waveform for voltage V1 in Fig. 2). The spikes at time of 0.1 to 0.7 µs in the laser pulse waveform are attributed to switching noise from the main discharge
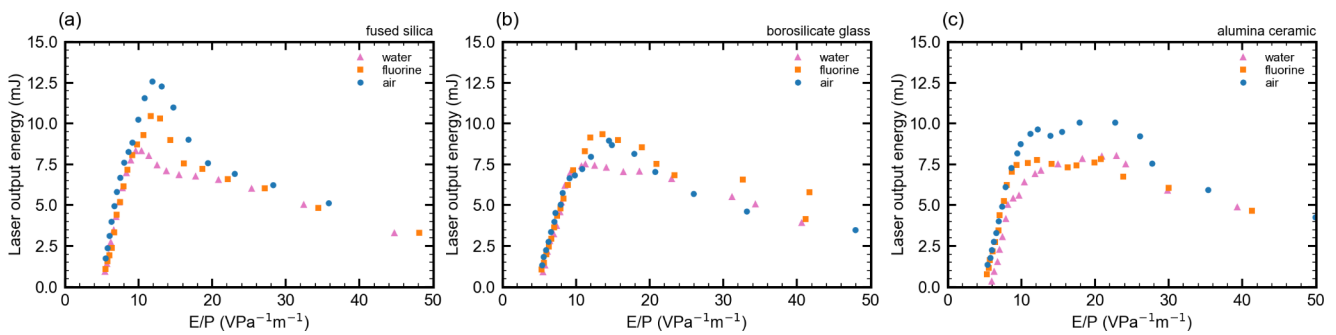
Fig. 5 Dependence of measured laser output energy on E/P with a discharge tube made of fused silica (**a**), borosilicate glass (**b**), and alumina ceramic (**c**). Pink triangles, orange squares, and blue circles correspond to pure water, fluorinated fluid, and air, respectively
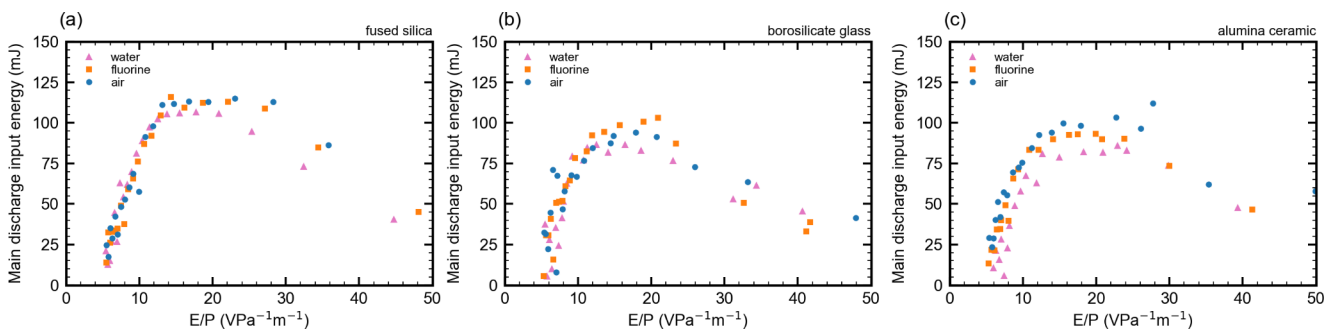

Fig. 6 Dependence of calculated main discharge input energy on E/P with a discharge tube made of fused silica (**a**), borosilicate glass (**b**), and alumina ceramic (**c**). Pink triangles, orange squares, and blue circles represent pure water, fluorinated fluid, and air, respectively

energy between E/P of 10.0 and 22.0. The highest laser output energy was observed at 8.3 mJ for pure water at an E/P of 10.4, 10.5 mJ for fluorinated fluid at an E/P of 11.6, and 12.6 mJ for air at an E/P of 11.8. For fused silica discharge tubes, air yielded the maximum laser output energy. Figure 5b illustrates the E/P dependence of laser output energy in borosilicate glass discharge tubes. The coolant material influenced the laser output energy within the range of E/P of 10.0 to 20.0. The highest laser output energy was 7.5 mJ for pure water at an E/P of 11.2, 9.3 mJ for fluorinated fluid at an E/P of 13.6, and 9.0 mJ for air at an E/P of 14.4. In borosilicate glass discharge tubes, the coolant that provided the highest laser output energy was fluorinated fluid. Figure 5c demonstrates the E/P dependence of laser output energy in alumina ceramic discharge tubes. The coolant material influenced the laser output energy between E/P of 8.0 to 30.0. The maximum laser output energy was 8.0 mJ for pure water at an E/P of 22.9, 7.8 mJ for fluorinated fluid at an E/P of 20.8, and 10.1 mJ for air at an E/P of 17.9. For alumina ceramic discharge tubes, air resulted in the highest laser output energy.

The discharge tube material and the coolant material influenced the laser output energy. Moreover, the discharge tube material also influenced how the laser output energy depended on the coolant material. The highest laser output energy, 12.6 mJ, was achieved with fused silica discharge

tubes and air coolant. Across all discharge tubes, laser output energy was lowest when using pure water as the coolant.

3.3 Effect on main discharge energy

We investigated how the discharge tube material and coolant material affected the main discharge input energy. This energy was calculated using voltage V1 and current I1. Figure 6a displays the E/P dependence of the main discharge input energy in fused silica discharge tubes. The coolant material influenced the main discharge input energy at E/P values of 12.0 and above. With pure water, the maximum main discharge input energy was approximately 106 mJ at E/P ranging from 13.8 to 20.8. For fluorinated fluids, the maximum main discharge input energy was approximately 113 mJ at E/P values of 14.3 to 27.2. With air, the maximum main discharge input energy was approximately 112 mJ at E/P values of 13.1 to 28.2. In fused silica discharge tubes, the coolant that yielded the highest main discharge input energy was fluorinated fluid. The maximum main discharge input energy remained nearly constant for all coolants, regardless of E/P. The energy supplied by the power supply was determined by the capacitance of its internal capacitor, with a maximum value of 125 mJ. Considering capacitance transfer loss and dielectric loss, it was assumed that all energy supplied by the power supply was consumed. In

Table 2 Conversion efficiency at E/P values that provided the maximum value of laser

discharge tube	coolant	laser output energy (mJ)	E/P (VPa^{-1}m^{-1})	main discharge input energy (mJ)	conversion efficiency (%)
fused silica	pure water	8.3	10.4	88.8	9.3
	fluorinated fluid	10.5	11.6	92.1	11.4
	air	12.6	11.8	97.9	12.9
borosilicate glass	pure water	7.5	11.2	84.5	8.9
	fluorinated fluid	9.3	13.6	94.3	9.9
	air	9.0	14.4	87.6	10.3
alumina ceramic	pure water	8.0	22.9	85.8	9.3
	fluorinated fluid	7.8	20.8	89.8	8.7
	air	10.1	17.9	98.1	10.3

a fused silica discharge tube, an increase in supplied energy from the power supply might raise laser output energy. Figure 6b illustrates the E/P dependence of the main discharge input energy in borosilicate glass discharge tubes. The coolant material influenced the main discharge input energy within the range of E/P from 12.0 to 24.0. For pure water, the maximum main discharge input energy was 84.5 mJ at E/P of 11.2. For fluorinated fluid, it peaked at 94.3 mJ with an E/P of 13.6, while for air, it reached 87.6 mJ at E/P of 14.4. In borosilicate glass discharge tubes, the coolant maximizing the main discharge input energy was fluorinated fluid. Figure 6c illustrates the E/P dependence of the main discharge input energy in alumina ceramic discharge tubes. The coolant material impacted the main discharge input energy at E/P of 22.0 and below. For pure water, the highest main discharge input energy recorded was 84.5 mJ at E/P of 11.2. For fluorinated fluid, it peaked at 94.3 mJ with an E/P of 13.6, while for air, it reached 87.6 mJ at E/P of 14.4. In alumina ceramic discharge tubes, the coolant maximizing the main discharge input energy was air.

The main discharge input energy was lowest with pure water as the coolant for all discharge tube materials. Both the discharge tube material and the coolant material influenced the main discharge input energy. Additionally, the discharge tube material affected how the main discharge input energy depended on the coolant material. In fused silica and borosilicate glass discharge tubes, the main discharge input energy showed no correlation with the permittivity of the coolant material. However, the permittivity of both the discharge tube and the coolant impacted the characteristic impedance of the discharge system. While the permittivity of the discharge tube and the coolant did not directly affect the main discharge energy, they did influence the characteristic impedance, which in turn affected the main discharge energy.

3.4 Discussion

As depicted in Sect. 3.2, the E/P ranges where the coolant material affects the laser output energy were E/P of 10.0 to 22.0 for a fused silica discharge tube, E/P of 10.0 to 20.0 for a borosilicate glass discharge tube, and E/P of 8.0 to 30.0 for an alumina ceramic discharge tube. As illustrated in Sect. 3.3, the E/P range where the coolant material influences the main discharge input energy was E/P of 12.0 and higher for a fused silica discharge tube, E/P of 12.0 to 24.0 for a borosilicate glass discharge tube, and E/P of 22 and lower for an alumina ceramic discharge tube. While the main discharge energy should affect the laser output energy, the range in which the coolant material impacted the laser output energy was narrower than the range affecting the main discharge energy. This suggests that there may exist an E/P range where the laser output energy was saturated relative to the main discharge energy.

The discharge tube material and coolant material could have also influenced the discharge distribution within the discharge tube. Table 2 lists the conversion efficiencies at E/P values where the maximum laser output energy was achieved for all combinations of discharge tube material and coolant material. These efficiencies were calculated based on the main discharge input energy and the laser output energy. Notably, the conversion efficiency calculations exclude the energy consumed by dielectric losses in the capacitor Cs. Both the discharge tube material and the coolant material impacted the conversion efficiency. Furthermore, the discharge distribution within the discharge tube, influenced by both the discharge tube and coolant materials, played a role in determining the laser gain distribution, thereby affecting the conversion efficiency.

4 Conclusion

In a longitudinally excited CO_2 laser with fast pulsed discharge, we investigated the impact of discharge tube material and coolant material on fast discharge and laser output energy. In a discharge tube with a coolant tube, a capacitance formed between the discharge tube and coolant affected the discharge. Both discharge tube and coolant material influenced the main discharge input energy. No

correlation between the permittivity of the coolant and the main discharge input energy was observed in fused silica and borosilicate glass discharge tubes. However, the characteristic impedance of the discharge system, determined by discharge tube and coolant permittivity, likely influenced the main discharge input energy. Laser output energy depended on the main discharge input energy, influenced by both discharge tube and coolant material. Additionally, laser output energy may have been influenced by discharge distribution in the tube, affected by discharge tube and coolant material. These findings serve as a reference for optimizing cooling systems for longitudinally excited CO$_2$ lasers with fast pulsed discharges. Future studies will aim to achieve high-energy, short-pulse repetition rate oscillation at a 10 kHz repetition rate.

Author contributions Y.K. wrote the manuscript text, prepared all figures, and preformed data analysis. S.W. carried out measurements. K.U. provided Supervision and Conceptualization. All authors reviewed the manuscript.

Declarations

Competing interests The authors declare no competing interests.

References

1. N. Menyuk, P.F. Moulton, Rev. Sci. Instrum. **51**, 216 (1980)
2. E. Arimondo, F. Casagrande, L.A. Lugiato, P. Glorieux, Appl. Phys. B **30**, 57 (1983)
3. K. Uno, K. Nakamura, T. Goto, T. Jitsuno, J. Infrared Millim. Terahertz Waves. **30**, 1123 (2009)
4. K. Uno, K. Dobashi, T. Akitsu, T. Jitsuno, Proc. SPIE 9266, 92661U (2014)
5. K. Uno, T. Jitsuno, Proc. SPIE 10811, 1081111(2018)
6. K. Uno, J. Li, H. Goto, T. Jitsuno, Proc. SPIE 10518, 105181Y(2018)
7. K. Uno, K. Yanai, S. Watarai, Y. Kodama, K. Yoneya, T. Jitsuno, Opt. Laser Technol. 152 (2022)
8. Y. Kodama, K. Yoneya, K. Uno, Appl. Phys. B **130**, 82 (2024)
9. G. Moeller, J.D. Rigden, Appl. Phys. Lett. **7**, 274 (1965)
10. C.K.N. Patel, P.K. Tien, J.H. McFee, Appl. Phys. Lett. **7**, 290 (1965)
11. I. Boscolo, P. Bernardini, Il Nuovo Cimento D **10**, 407–415 (1988)
12. A.K. Nath, V.S. Golubev, Pramana J. Phys. **51**, 463–479 (1998)